International Journal of Applied Mathematics, Electronics and Computers 8(4): 209-213, 2020

e-ISSN: 2147-8228

INTERNATIONAL JOURNAL OF APPLIED MATHEMATICS ELECTRONICS AND COMPUTERS

www.dergipark.org.tr/ijamec

International Open Access

Volume 08
Issue 04

December,2020

Research Article

UDE Based Robust Control of Grid Tied Inverters

Akın Uslu [a,*]

[a]*Department of Electrical and Electronics Engineering, Engineering Faculty, Alparslan Türkeş Science and Techmology University, Adana, Turkey*

ARTICLE INFO

Article history:
Received 01 October 2020
Accepted 21 October 2020
Keywords:
Uncertainty
Disturbance
Robust Control
Inverters

ABSTRACT

In this paper, a modified (proportional-integral) PI control is suggested to improve current tracking performance of three-phase grid-tied inverters (GTI). Presence of the L filter between inverter and grid, makes complex to design a controller with proper parameters, due to characteristics of the filter. Clasical PI control depends on an accurate dynamical model, thus its performance is deteriorated by parametric uncertainties, unmodelled dynamics and external disturbances, when operating conditions affect the filter parameters. To solve this problem, uncertainty and disturbance estimator based PI current control approach is proposed for grid-tied inverters, which provides robustness against to parametric perturbations. An UDE based observer that has been adopted into the PI current loop is used to eliminate lumped disturbances and the steady-state tracking error of current states, which can enhance the robustness of the control performance. Then, parameter design method, stability and robustness analysis are explored and presented. Performance comparison among the clasical PI and proposed control scheme. Efficacy and performance of the proposed approach are carried out by simulations and experiments. Experimental results show that effectiveness of the suggested control method against parametric uncertainties and disturbances are succesfully validated. Besides, the precise current tracking performance with zero steady state error has been reached.

1. Introduction

Grid-tied inverter (GTI) has a very important role in ensuring high quality current injected into the grid, have progressively been adopted in renewable energy systems [1], distributed generation, battery storage systems, and uninterruptible power supplies (UPSs), hybrid electric mobility, smart grids, etc. To obtain pure sine wave, an L grid filter is usually placed as an interface between inverter and power grid to reduce high frequency current harmonics[1]. However, when the grid filter varies, due to temperature, saturation etc., closed loop control performance may be adversely affected and output current is contaminated with harmonics caused by parametric uncertainties. In addition to, the unmodeled dynamics like disturbances and dead-time, can deteriorate the control performance and stability. For the current control of GTI, many strategies have been applied, such as proportional–integral (PI) control [2], proportional–resonant (PR) control [3], and repetitive control (RC) [4], etc. Although these controllers are good to eliminate steady state error, they have lack about robustness.

For robustness concern of the GTI, there have been a number of conventional strategies, such as adaptive control [5], sliding mode control (SMC)[6], disturbance observer based control (DOBC) [7], active disturbance rejection control (ADRC) [8] and uncertainty and disturbance estimator (UDE) based control[9]. Among those methods, UDE based control has become very attractive research point because of ıt gives a new solution for disturbance rejection and also its good reference tracking performance[10].

The main principle of the UDE based control scheme is estimating the lumped terms, including parametric uncertainties and disturbances by using state measurements and a low-pass filter with a appropriate

* Corresponding author. E-mail address: *auslu@atu.edu.tr*
DOI: 10.18100/ijamec.803545

bandwidth. Then, estimated lumped disturbance could be adopted to the control action to reject against to disturbances. UDE based control doesn't require an accurate model of the system and provides the decoupled control design for desired model an filter bandwidth [11]. Due to its superior performance, UDE based control scheme was applied to control of piezoelectric stages [12], wind turbines [13], motor drives [14] and power converters [15]. However, to our best knowledge, UDE-based control of GTI has been represented on few studies and it should be developed [16],[17].

In this paper, a UDE-based control scheme is forming PI controller for GTI with L filter is proposed. By using desired model and low-pass filter parameters, a simple and practical PI control approach converted from UDE based control is composed.

2. Modeling of the GTI

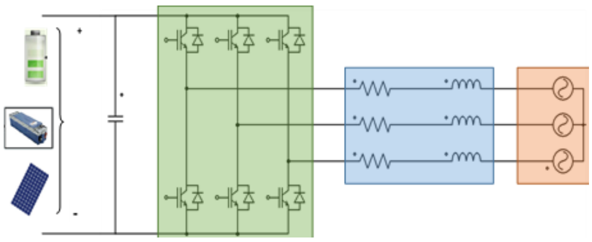

Fig.1 Grid Tied Inverter System

The schematic diagram of the grid-tied inverter system studied for this work is depicted in Fig. 1. The control of grid side currents and dc-link voltage of inverter represents the main purpose of this paper. Following [18], differential equations that describe the nonlinear affine form of the dynamics of dc-link voltage and grid-side inverter currents, in the synchronous rotating reference frame (SRF), can be defined as follows:

$$L\frac{di_d}{dt} = -Ri_d + \omega L i_q + u_d - v_{gd} \tag{1}$$

$$L\frac{di_q}{dt} = -Ri_q - \omega L i_d + u_q - v_{gq} \tag{2}$$

$$C\frac{dV_{dc}}{dt} = -\frac{3}{2V_{dc}}[e_d I_d + e_q I_q] \tag{3}$$

Where, R and L are grid side filter inductance and resistance respectively and C represents dc-link capacitor. Angular frequency of the grid voltage is denoted as ω, which is obtained by phase locked loop (PLL) scheme. Grid voltage (e_d, e_q), control functions (u_d, u_q), and grid side currents (I_d, I_q), are all obtained in dq synchronous rotating frame

Before designing the proposed UDE-based PI current control strategy, parameter uncertainties of grid currents channels of the dynamic model given in (1)-(3) must be derived as follows

$$\frac{di_d}{dt} = -\frac{R}{L}i_d + \omega i_q + \frac{u_d}{L} - \frac{v_{gd}}{L} + d_{id} \tag{4}$$

$$\frac{di_q}{dt} = -\frac{R}{L}i_q - \omega i_d + \frac{u_q}{L} - \frac{v_{gq}}{L} + d_{iq} \tag{5}$$

Where the parameters R, L and C are nominal values, d_{id} and d_{iq} represents lumped disturbances and parametric variations

3. Besed PI Control Law

Dynamic equations of GTI system given in (4)-(5) can be rewritten as the following state space compact form:

$$\dot{\boldsymbol{x}}(\boldsymbol{t}) = \boldsymbol{Ax}(\boldsymbol{t}) + \boldsymbol{Bu}(\boldsymbol{t}) + \boldsymbol{Fx}(\boldsymbol{t}) + \boldsymbol{G} + \boldsymbol{d} \tag{6}$$

With

$$A = \begin{bmatrix} \frac{-R}{L} & 0 \\ 0 & \frac{-R}{L} \end{bmatrix} \qquad B = \begin{bmatrix} \frac{1}{L} & 0 \\ 0 & \frac{1}{L} \end{bmatrix}$$

$$F = \begin{bmatrix} 0 & \omega \\ -\omega & 0 \end{bmatrix} \qquad G = \begin{bmatrix} \frac{e_d}{L} \\ \frac{e_q}{L} \end{bmatrix}$$

Where, $\boldsymbol{x} = [\boldsymbol{I_d}\ \boldsymbol{I_q}]^{\boldsymbol{T}}$ is state vector, , $\boldsymbol{u} = [\boldsymbol{u_d}\ \boldsymbol{u_q}]^{\boldsymbol{T}}$ is control input functions, and $\boldsymbol{d} = [\boldsymbol{d_{id}}\ \boldsymbol{d_{iq}}]^{\boldsymbol{T}}$ is parametric uncertainty and disturbance vector

Assume, desired closed-loop dynamics of GTI system can be defined with reference model as

$$\dot{\boldsymbol{x}}_{\boldsymbol{d}} = \boldsymbol{A_d x_d} + \boldsymbol{B_d c} \tag{7}$$

Where, $x_d = [I_{dm}\ I_{qm}]^T$ is desired state vector, $c = [I_d^r\ I_q^r]$ is the reference command input vector. A_d is desired state matrix, and $B_d$is desired control vector. In order to get desired specifications of the closed loop system, A_d and B_d matrix coefficients are selected to meet desired bandwith. Decoupled first order system with grid current bandwith τ_{id} and τ_{id} can be described as

$$A_d = \begin{bmatrix} -\tau_{id} & 0 \\ 0 & -\tau_{iq} \end{bmatrix} \ and\ B_d = \begin{bmatrix} \tau_{id} & 0 \\ 0 & \tau_{iq} \end{bmatrix}$$

Control law $u(t)$ is to ensure that $x(t)$ asymptotically tracks the desired state x_d and, idealy tracking error, i.e.,

$$\boldsymbol{e}(\boldsymbol{t}) = \boldsymbol{x_d}(\boldsymbol{t}) - \boldsymbol{x}(\boldsymbol{t}) \tag{8}$$

converges to zero. One method to design a control law $u(t)$ is to satisfy the condition for the error dynamics as

$$\dot{\boldsymbol{e}} = \boldsymbol{A_d e} \tag{9}$$

By equating (6) and (9) results in

$$\boldsymbol{A_d x}(\boldsymbol{t}) + \boldsymbol{B_d c}(\boldsymbol{t}) - \boldsymbol{Ax}(\boldsymbol{t}) - \boldsymbol{Bu}(\boldsymbol{t}) - \boldsymbol{Fx}(\boldsymbol{t}) - \boldsymbol{G}$$

$$-\boldsymbol{d} = \boldsymbol{A_d e} \tag{10}$$

Then, the control law can be obtained as

$$u(t) = B^{-1}[\,A_d x + B_d c - Ax - Fx - G - d \quad (11)$$

Based on (6), uncertainty terms and external disturbances d, which can be defined as

$$d = \dot{x}(t) - Ax(t) - Bu(t) - Fx(t) - G \quad (12)$$

Following the control guidelines in [11], d can be approximated by

$$\hat{d}(t) = d(t) * g_f(t) \quad (13)$$

where " $*$ " is the convolution operator and $g_f(t)$ is the strictly proper low-pass filter which is used to estimate lumped term d . By replacing $d(t)$ with $\hat{d}(t)$, the equations (11) becomes

$$u(t) = B^{-1}[\,A_d x + B_d c - Ax - fx - G - d * g_f(t \quad (14)$$

Then by substituting (12) into (14) results in

$$u(t) = B^{-1}[\,A_d x + B_d c - Ax - fx - G -$$

$$[\dot{x}(t) - Ax(t) - Bu(t) - fx(t) - G] * g_f(t)] \quad (15)$$

Rearranging control function u(t) in (15) and taking the Laplace transform, the control law in s-domain can be derived in equation (16). Where $G_f(s)$ is represented as the Laplace transform of $g_f(t)$.

Frequency characteristic of $G_f(s)$ filter needs to have large enough bandwith, unity steady state gain and zero phase shift over the spectrum of uncertainty term d. An accurate estimation of filter bandwidth is difficult due to deadtime of the inverter and control delay. Hence, first order low-pass filter is often preferred as follows

$$G_f(s) = \frac{\tau_f}{sI_{2x2} + \tau_f} \quad (17)$$

Where, $\tau_f = [\tau_{fd}\ 0; 0\ \tau_{fq}]$is bandwidth of the $G_f(s)$. By substituting (17) into (16) UDE based control action can be obtained as follows

$$u(s) = B^{-1}[A_d x_d(s) + B_d c(s) - (Ax(s) + Fx(s)$$

$$+G) - K_p e(s) - K_i e(s)] \quad (18)$$

Where,

$$K_p = (\tau_f - A_d) \textit{ and } K_i = \frac{\tau_f}{sI_{2x2}} A_d$$

Equation (18) shows that control law consist of PI regulator to make the tracking error zero, feedforward compansator for desired transients and negative model to cancel the known dynamics. From equation (18), PI parameters don't need to have the exact filter parameters. This allows practically adjusting the two τ_f and τ_d bandwidths for the PI parameter design problem. Overall control daigram is shown in Figure 2.

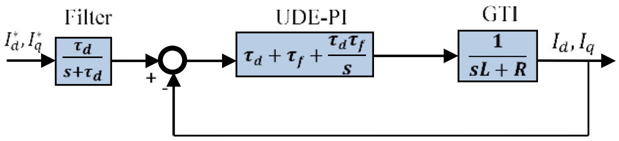

Figure 2. Block diagram of UDE-PI based control system

Substituting (16) into the laplace transform of (6), decoupled structure of the system response can be derived as follows:

$$x(s) = \frac{\tau_d}{s + \tau_d} c + \frac{1}{s + \tau_d}\frac{s}{s + \tau_f} d \quad (19)$$

It is clear that, the parameter design problem can be considered as adjustment of the two bandwidths, which are τ_d and τ_f. For fixed value of τ_d , which is designed according to desired transient specifications, closed loop performance can be adjusted with τ_f until to meet desired disturbance attenuation. For larger values of damping τ_d, the dominant poles move far from the real axis, which can cause to underdamped response with large overshoot.

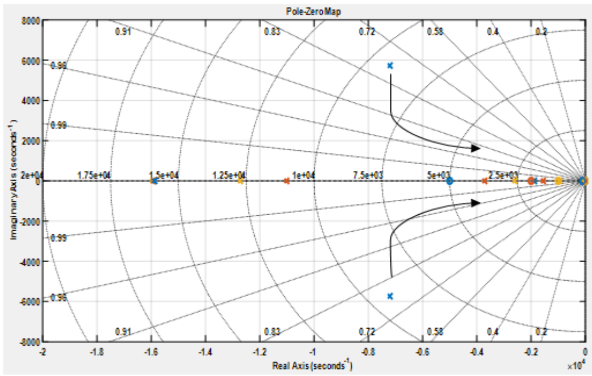

Figure 3. Pz map of the closed loop system

Besides Fig. 3 shows the closed loop poles of the system (19) for the different bandwidth τ_f. We can observer that the dominant poles get close to the imaginary axis as the bandwidth of the filter increased. Thus, the time constant of $G_f(s)$ filter should not choose too small to avoid instability.

4. Simulation Studies

In order to validate the proposed UDE based PI current control method in Fig 4, some of simulations studies were performed on RL filtered GTI system. Electrical parameters of the GTI system are given in table 1. Clasical PI control strategy based on synchronous reference is selected as base controller to compare the proposed control approach as shown in Fig 5. Control parameters are summarized in table 2 according to same closed loop performance for feasible comparision. Bandwidth of outer PI loop for dc link voltage regulation was selected as 20 rad/s for both methods.

$$u(s) = B^{-1}[\,(A_d x(s) + B_d c(s))\frac{1}{(1-G_f(s))} - (Ax(s) + Fx(s) + G) - sx(s)\frac{G_f(s)}{(1-G_f(s))}] \tag{16}$$

Table1 Electrical parameters for GTI system

Filter inductor L	10mh
Filter resistor R	3 ohm
Dc link capacitor C	1mf
Grid frequency	50 hz
Dc link voltage reference	500 V
Phase-to-neutral voltage	100 V
Switching frequency	10 khz

Table 2 Control parameters

τ_{id}, τ_{iq}	(1000,1000)
τ_{fd}, τ_{fq}	(3000,3000)
K_{pi}, K_{ii}	(1,1000)
$\boldsymbol{K_{p\_dci}}, \boldsymbol{K_{i\_dc}}$	(1,20)

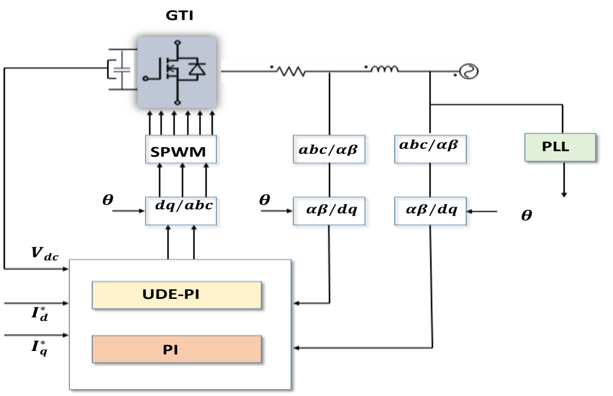

Figure 4. Shematic diagram of GTI system with SRF

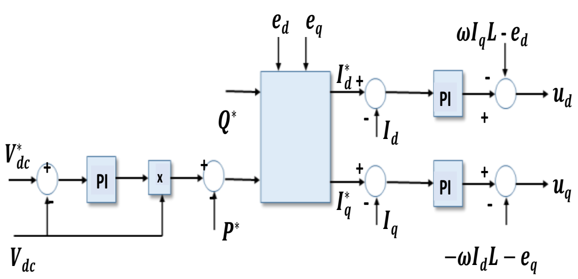

Figure 5. Shematic diagram of PI control with SRF

Dynamic response of the proposed control strategy was tested against to reactive power change applied to grid. Figure 6 shows active and reactive power references, besides figure 7 shows injected grid current and voltage.Active power is kept 1kw whereas reactive power is suddenly cahnged from 500 Var to 0. As shown in Figure 7, proposed control strategy can response to the reactive power change with fast and zero steady state error.

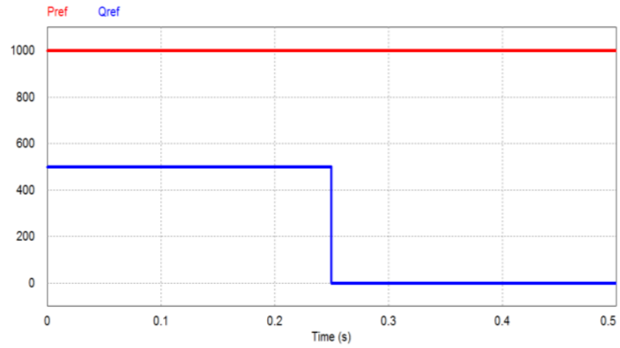

Fig 6 Active and reactive power reference variations

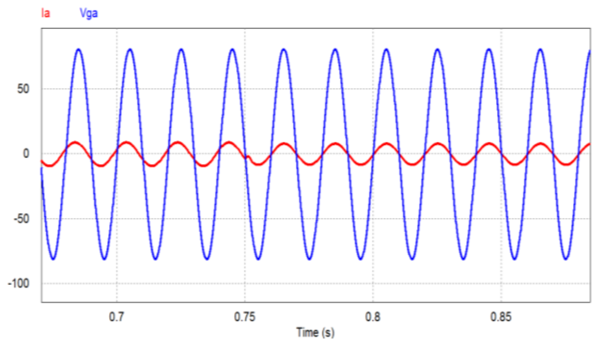

Fig 7 Injected current and grid voltage

Proposed and classical PI control performance was compared against to parametric mismatch shown in Fig 8. The simulation was conducted with deviation of L as %150L. It can be observed that a small steady state error with classical PI control and large owershoot. However parametric mismatch has very small effect on the performance of UDE based PI control as shown in Fig 9.

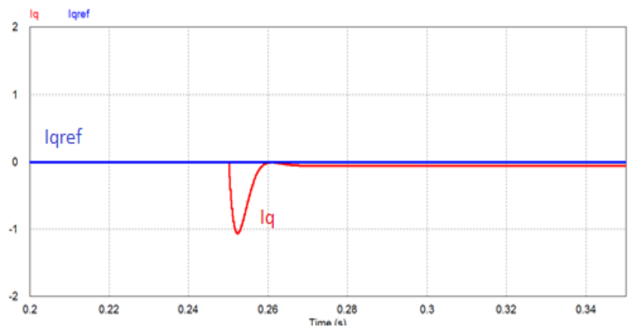

Figure 8. Dynamic response of PI control with %150L

Figure 10. shows dynamic response I_q current under %50 L parametric mismatch. Classical PI control has small offset error while tracking reference current, wheres proposed control shows fast transient response and zero steady state error under parametric uncertainties.

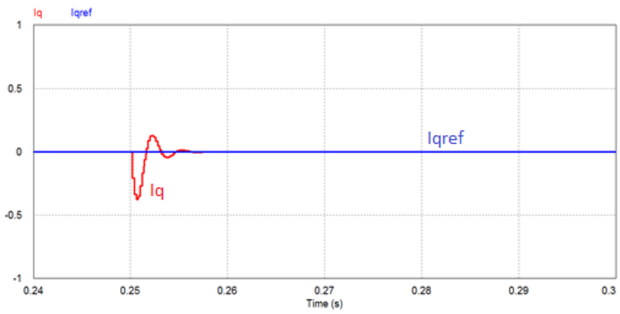

Figure 9. Dynamic response of UDE- PI control with %150L

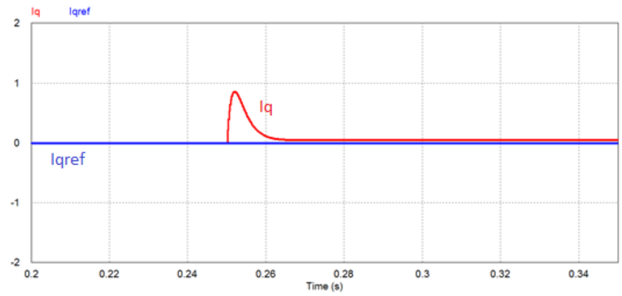

Figure 10. Dynamic response of UDE- PI control with %50 L

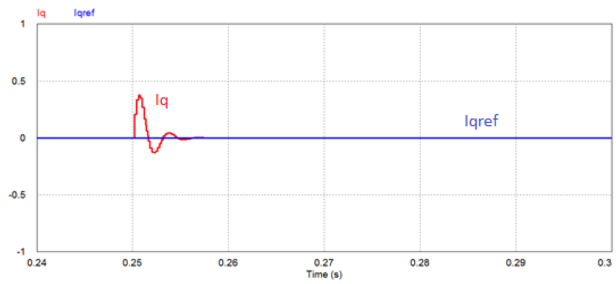

Figure 11 Dynamic response of UDE- PI control with %50 L

5. Conclusion

This paper proposed a proportional-Integral (PI) control strategy based uncertainty and disturbance estimator (UDE) for three phase GTI systems. With the poposed control method, an improved disturbance attenuation was achieved. Deviations of grid filter parameters and operating conditions make hard to choose control parameter with satisfied performance. This paper presents a simplified parameter selection approach for PI control by using two parameters which are associated with bandwidths of desired closed loop and lumped uncertainty repectively. Also this stategy enable two degree of freedom control. Simulation studies demonstrate that proposed controller performed better performance than conventional PI controller in terms of robustness and dynamic performance

Author's Note

Abstract version of this paper was presented at 9th International Conference on Advanced Technologies (ICAT'20), 10-12 August 2020, Istanbul, Turkey with the title of “UDE Based Robust Control of Grid Tied Inverters”.

References

[1] M. Lindgren and J. Svensson, “Control of a voltage-source converter connected to the grid through an LCL-filter-application to active filtering,” in Proc. IEEE Power Electron. Spec. Conf., May 1998, pp. 229–235.

[2] W. Li, X. Ruan, D. Pan, and X. Wang, “Full-feedforward schemes of grid voltages for a three-phase LCL-type grid-connected inverter,” IEEE Trans. Ind. Electron., vol. 60, no. 6, pp. 2237–2250, Jun. 2013.

[3] Q. Zhao, Y. Ye, G. Xu, and M. Zhu, “Improved repetitive control scheme for grid-connected inverter with frequency adaptation,” IET Power Electron., vol. 9, no. 5, pp. 883–890, Apr. 2016.

[4] R. Teodorescu, F. Blaabjerg, M. Liserre, and P. C. Loh, “Proportional resonant controllers and filters for grid-connected voltage-source converters,” in Proc. Elect. Power Appl., vol. 153, no. 5, pp. 750–762, Sep. 2006.

[5] S. Tong, Y. Li, and S. Sui, “Adaptive fuzzy tracking control design for SISO uncertain nonstrict feedback nonlinear systems,” IEEE Trans. Fuzzy Syst., vol. 24, no. 6, pp. 1441–1454, Dec. 2016

[6] N. Kumar, T. K. Saha, and J. Dey, “Sliding-mode control of PWM dual inverter-based grid-connected PV system: Modeling and performance analysis,” IEEE J. Emerg. Sel. Topics Power Electron., vol. 4, no. 2, pp. 435–444, Jun. 2016.

[7] E. Sariyildiz and K. Ohnishi, “Stability and robustness of disturbanceobserver- based motion control systems,” IEEE Trans. Ind. Electron., vol. 62, no. 1, pp. 414–422, Jan. 2015.

[8] J. Han, “From PID to active disturbance rejection control,” IEEE Trans. Ind. Electron., vol. 56, no. 3, pp. 900–906, Mar. 2009.

[9] B. Ren, Q.-C. Zhong, and J. Dai, “Asymptotic reference tracking and disturbance rejection of UDE-based robust control,” IEEE Trans. Ind. Electron., vol. 64, no. 4, pp. 3166–3176, Apr. 2017.

[10] J. Ren, Y. Ye, G. Xu, Q. Zhao, and M. Zhu, “Uncertainty-and-disturbanceestimator- based current control scheme for PMSM drives with a simple parameter tuning algorithm,” IEEE Trans. Power Electron., vol. 32, no. 7, pp. 5712–5722, Jul. 2017.

[11] Q.-C. Zhong, A. Kuperman, and R. K. Stobart, “Design of UDE-based controllers from their two-degree-of-freedom nature,” Int. J. Robust Nonlinear Control, vol. 21, no. 17, pp. 1994–2008, Nov. 2011.

[12] J. Chen, B. Ren, and Q.-C. Zhong, “UDE-based trajectory tracking control of piezoelectric stages,” IEEE Trans. Ind. Electron., vol. 63, no. 10, pp. 6450–6459, Oct. 2016.

[13] B. Ren, Y.Wang, and Q.-C. Zhong, “UDE-based control of variable-speed wind turbine systems,” Int. J. Control, vol. 90, no. 1, pp. 137–152, 2017.

[14] J. Ren, Y. Ye, G. Xu, Q. Zhao, and M. Zhu, “Uncertainty and disturbance estimator-based current control scheme for PMSM drives with a simple parameter tuning algorithm,” IEEE Trans. Power Electron., vol. 32, no. 7, pp. 5712–5722, Jul. 2017,

[15] I. Aharon, D. Shmilovitz, and A. Kuperman, “Robust output voltage control of multimode non-inverting DC-DC converter,” Int. J. Control, vol. 90, no. 1, pp. 110–120, 2017.

[16] S. Y. Gadelovits, Q.-C. Zhong, V. Kadirkamanathan, and A. Kuperman, “UDE-based controller equipped with a multi-band-stop filter to improve the voltage quality of inverters,” IEEE Trans. Ind. Electron., vol. 64, no. 9, pp. 7433–7443, Sep. 2017.

[17] Y. Ye and Y. Xiong, “UDE-based current control strategy for LCCL-type grid-tied inverters,” IEEE Trans. Ind. Electron., vol. 65, no. 5, pp. 4061– 4069, May 2018.

[18] [18] R. Errouissi, M. Ouhrouche, W.-H. Chen, and A. M. Trzynadlowski, “Robust nonlinear predictive controller for permanent-magnet synchronous motors with an optimized cost function,” IEEE Trans. Ind. Electron., vol. 59, no. 7, pp. 2849–2858, Jul. 2012